

## Delineating a detailed mountain ecosystem using spatial statistics: A case study in Kodil Watershed, Menoreh-Sumbing Mountain, Central Java, Indonesia

Rina Purwaningsih<sup>1</sup> , Junun Sartohadi<sup>2\*</sup> , Guruh Samodra<sup>3</sup> , Cristopher Gomez<sup>4</sup> 

<sup>1</sup> Department of Environmental Science, The Graduate School, Universitas Gadjah Mada, Yogyakarta, 55281, Indonesia

<sup>2</sup> Department of Soil Science, Faculty of Agriculture, Universitas Gadjah Mada, Yogyakarta, 55281, Indonesia

<sup>3</sup> Department of Environmental Geography, Faculty of Geography, Universitas Gadjah Mada, Yogyakarta, 55281, Indonesia

<sup>4</sup> Faculty of Maritime Science, Kobe University, Japan

\* Corresponding author's e-mail: junun@ugm.ac.id

### ABSTRACT

Mapping mountain ecosystems is needed for local planning. Ecosystem boundaries are influenced by interrelated physical and environmental factors rather than singular physical features. Tropical mountain landscapes exhibit diverse surface patterns, impacting their terrestrial ecological systems. Using river network data and digital terrain models (DTMs), we delineated ecosystem groups based on seven surface parameters: river order, channel sinuosity, elevation, slope, aspect, roughness index, and curvature. A multivariate clustering method identified ecosystem groups with similar attributes, further clarified using geological and land cover maps to account for surface and subsurface material variations and their processes. Our analysis identified five distinct ecosystem units: the young Sumbing volcanic peak, old Sumbing volcanic peak, old Sumbing volcanic slope, transitional volcanic, and old Menoreh volcanic ecosystems. The parameters that have a strong influence in limiting these units are elevation, slope, curvature, and roughness. Despite being part of the same mountain range, these ecosystems exhibit markedly different physical land characteristics. The surface-boundary-based delineation method provides a practical approach to defining mountain ecosystems, aligning spatial planning with land capacity and ecosystem service provisioning. By incorporating insights from river flow patterns and DTMs, this method captures the complexity of land surfaces shaped by past volcanic-tectonic activity and ongoing erosion-deposition processes. The resulting spatial boundaries reflect both current natural capital and dynamic limiting factors, demonstrating its potential for effective and detailed landscape management in complex mountainous regions.

**Keywords:** mountain ecosystem, terrestrial ecological systems, land surface parameters, spatial statistic, local planning.

### INTRODUCTION

Mountain ecosystems are unique due to their distinct physiography features. Delineating mountain ecosystems based on homogeneous landscapes and their spatial arrangement is a critical approach in understanding and managing these complex environments. This method involves identifying areas with similar ecological and geomorphological characteristics, considering factors like elevation, slope, aspect, and river patterns, and how they

spatially relate to each other across the landscape (Grêt-Regamey and Weibel, 2020; Mac-Millan et al., 2004). Homogeneous landscapes in mountain ecosystems refer to areas where environmental conditions, such as climate, soil, and topography, are consistent and distinct from surrounding regions (Birkeland, 2014; Körner, 2021; West, 2001). These homogeneous areas often support specific plant and animal communities adapted to the local conditions. Delineation based on these landscapes helps in identifying ecological units that are essential

for conservation and management (Cullingham et al., 2019; Weiss and Walsh, 2009).

The spatial arrangement of these homogeneous landscapes is crucial for understanding ecosystem connectivity, ecological processes, and biodiversity patterns (Chen, 2002). Mountain ecosystems are often characterized by sharp gradients and complex topographies, which create a mosaic of microhabitats. Analysing the spatial arrangement of these homogeneous landscapes allows for the identification of ecological corridors, barriers, and zones of ecological transition, which are vital for species movement and ecosystem resilience (Fouedjio and Arya, 2024; Zhou and Song, 2021).

Ways to identify mountain ecosystems, especially ecosystem services based on spatial data, are widely used through remote sensing and GIS (Germino et al., 2001; Grêt-Regamey et al., 2008; Li et al., 2006). Land surface morphology is an easily recognized and measurable parameter (Minár and Evans, 2008; Tarolli, 2014). Spatial data, especially terrain data that can be processed into land surface data, is now widely available and easily accessible. In Indonesia, official national topographic data of fairly good quality is available, and the derived data can be used to analyze land surface characteristics (Apriadsa et al., 2019; Lauder et al., 2023). This study specifically discusses how national data can be simply and easily used to identify mountain ecosystem boundaries.

Digital terrain models (DTM) and river networks as two key surface parameters characterized by distinct attributes that can be categorized to recognize mountain ecosystem. DTMs provide detailed and accurate terrain information essential for precise boundary delineation (Skouliki-dis, 2021). These models help in capturing the intricate topography of mountainous regions. The spatial arrangement of river networks across the landscape may play a role in the delivery of riverine ecosystem services, highlighting the need to consider river network geometry in the delineation of ecosystem boundaries (Karki et al., 2023). The similarity of these surface parameters is statistically analyzed, informed by a comprehensive understanding of the study area and available data (Weiss and Walsh, 2009). Terrain and river datasets with a resolution of 12.5 m offer valuable spatial information for modelling mountain ecosystem units (Aspinall and Pearson, 2000; Grêt-Regamey et al., 2012).

Apart from being characterized by its physiography, the mountain ecosystem is a unique land

ecosystem that has different biodiversity characteristics and socio-economic characteristics. (Tefera et al., 2024). The impact of sub-surface material information and land cover on the existing surface dynamics of a mountain ecosystem is influenced by various factors such as climate change and anthropogenic activities. Geological structures, such as fault zones and weathered zones, significantly impact the hydrological dynamics of mountain ecosystems. Identifying these structures helps in understanding the baseflow and catchment management (Marti et al., 2023). The structural manifestation of mountain geodynamics, including relief production and landscape evolution, is essential for understanding surface processes like erosion, deposition, and tectonic activities (Bishop and Dobrevá, 2017). Altitudinal gradients and land use types significantly influence species assemblages and functional diversity, shaping ecological patterns across mountain landscapes (García-Navas et al., 2020).

Mountain ecosystems are highly sensitive and vulnerable to change due to various human pressures and natural processes (Patru-Stupariu et al., 2020). Land use land cover (LULC) patterns categorize different types of land cover such as forest, grassland, shrubland, agricultural land, and built-up areas (Patley et al., 2024). Quantitative approaches to ecosystem service assessment rely on suitable indicators, and land use land cover can be used as an appropriate proxy. Monitoring these changes requires integrating land cover data with digital terrain models (DTMs), which allows for a detailed assessment of mountain ecosystems. This integration not only facilitates the tracking of ecological processes but also helps quantify the impact of environmental changes on land cover dynamics (Patley et al., 2024). Furthermore, analyzing the relationship between sub-surface material and land cover, significantly influences the dynamics of mountain ecosystems by impacting biodiversity, ecological processes, and ecosystem services.

## MATERIAL AND METHOD

### Area of study

The research was conducted on a section of volcanic slope within 113,6 kilometers square of the boundaries of the Kodil Watershed, located between coordinates -7.6251, 110.0748 and -7.5652, 110.0880. Geological mapping based

on information from sheets 1407-5, 1408-2, and 1409-2 indicates that the study area encompasses several geological formations, including Sumbing Young Volcanic Deposit (Qsm), Sumbing Old Volcanic Deposit (Qsmo), Bemmelen Formation (Tmok), and Sentolo Formation (Tmps). Despite small, the study area was selected to examine the diversity of ecosystem units shaped by the geology of the Southern Zone of Java Island (Figure 1).

The physiographic conditions of Java Island are generally divided into three landscape zones: the northern zone, the central zone, and the southern zone (Pannekoek, 1949). The Southern Zone is specifically dominated by old volcanic rocks, forming hilly and mountainous reliefs. During the Miocene, volcanic breccia in this zone was overlain by limestone deposits and shallow marine facies. These limestone deposits create a distinct relief that differs from the areas dominated by old volcanic rocks (Belyanin, 2021; Clements et al., 2009; Saputra et al., 2018). The Southern Zone of Java, characterized by uplifted southern mountains, Cenozoic volcanic arc rocks, and karst landscapes like the Gunung Sewu area, features a southward-sloping block mountain range with plateaus; this region, shaped by significant tectonic activity including thrusting and faulting that displaced volcanic arc rocks northward, transitions into the Central Zone with weakly folded old volcanic rocks, while its karst areas face water supply challenges due to their unique geological conditions (Oberle et al., 2016; Van Bemmelen, 1949).

The variety of subsurface conditions in the southern zone of Java Island needs to be easily identified through its surface characteristics. This study examines how these geological settings influence surface parameters and shape the ecosystems within the region (Antonelli et al., 2018).

The findings aim to offer a more comprehensive understanding of mountain ecosystem units within this volcanic landscape.

## Data source and processing

### DTM derivation

The primary data source for this study is the Indonesia Topographic Map at a 1:25,000 scale, which provides detailed topographic information, including contour lines with a 12.5-meter contour interval (CI). A DTM is generated from these contours through interpolation, offering a continuous elevation surface representation of the study area. This DTM serves as the foundational dataset for subsequent terrain and hydrological analyses (Šamanović et al., 2016). From the DTM, several critical terrain attributes are derived, including aspect, topographic position index (curvature), elevation, roughness, and slope.

Several key terrain attributes are derived from the DTM to assess various land characteristics. These attributes include aspect, which indicates the compass direction a slope faces and influences microclimate conditions and vegetation patterns (Salvacion, 2016). The Topographic Position Index (curvature) identifies the landscape position (e.g., ridge, valley, slope) for each point in the area, providing insights into landform processes (Giano et al., 2020). Elevation data supplies height information above sea level, essential for modeling elevation-dependent phenomena. Roughness quantifies terrain variability, indicating landscape ruggedness, which can affect land stability (Sathyamoorthy, 2009). Slope data, representing terrain incline, is vital for evaluating erosion potential and runoff behavior, impacting both ecological and hydrological systems (Zhang et al., 2018).

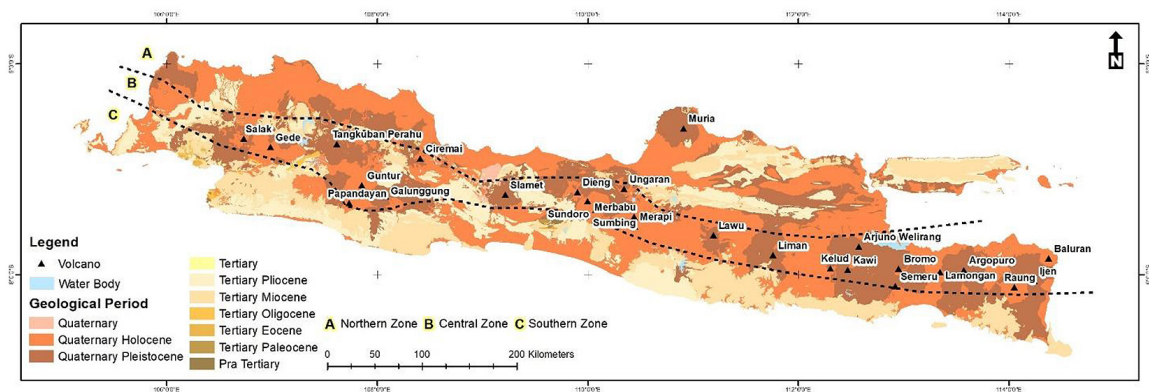


Figure 1. Map of the physiographic zones of Java Island where the study site is situated along the southern zone of Java

*River channel analysis*

River channels are extracted from the topographic map using the DTM, identifying flow paths and delineating the river networks. The river network hierarchy is established using river order classification based on the Strahler stream order system (Mileyko et al., 2012; Prskalo, 2010). Channel Sinuosity measures the degree to which a river meanders across the landscape, calculated as the ratio of the river’s channel length to the straight-line distance between two points along the river (Lane et al., 2017).

*Land use land cover identification*

The land cover of the study area was identified using a freely accessible data source, Planet-NICFI Imagery 2024 with 4.77 meters spatial resolution. The interpretation of land cover was performed using supervised classification in ArcGIS Pro, employing the Maximum Likelihood classifier. This classification process resulted in nine main land cover classes: forest, dryland agriculture, horticultural fields, bare land, mixed gardens, paddy fields, houses, water bodies, and roads.

*Grouping land surface parameters based on attribute similarity*

To effectively apply the methodology for grouping land surface parameters based on attribute similarity, it is essential to classify the data into distinct classes, as illustrated in the provided table (Table 1). The classification involves organizing terrain and hydrological attributes into specific ranges or categories that

reflect their spatial distribution and variability across the landscape. For river order, channel sinuosity, elevation, slope, aspect, roughness index, and topographic position index (curvature), each parameter is divided into several classes. River order is categorized from 1<sup>st</sup> to 4<sup>th</sup> order, with corresponding ranges of channel sinuosity (CS), which indicates the degree of river meandering. Elevation is classified into multiple intervals ranging from below 200 meters to over 2200 meters. Slope is similarly divided, beginning with flat terrain (0–1%) and extending to very steep slopes (>60%).

Aspect is categorized based on the cardinal directions, which influence microclimates and vegetation patterns. Roughness index and curvature are also segmented into specific ranges that capture the variability in terrain texture and landscape position. Lastly, land use land cover is categorized into 9 classes. These classes provide a structured way to analyze and compare different land surface characteristics, which is crucial for further spatial analysis and the identification of homogeneous zones within the study area. This classification serves as the foundation for conducting spatial statistical analysis, ensuring that each land surface parameter is appropriately grouped based on its attributes.

To achieve this grouping, spatial statistical techniques using multivariate clustering help to identify patterns and similarities within the data, facilitating the classification of the landscape into homogeneous zones. Multivariate Clustering finds natural clusters of features based solely on feature attribute values (Kang et al., 2022; Peeters

**Table 1.** Seven land surface parameter classes

River order	Channel sinuosity	Elevation [m]	Slope [%]	Aspect	Roughness index	Curvature
1 <sup>st</sup> Order	SR<1	<200	0–1 [flat]	East	0–0.211	-27.297–[-6.603]
2 <sup>nd</sup> Order	SR 1.1 –1.5	200–400	1–5 [gently sloping]	Flat	0.211–0.343	-6.603–[-2.841]
3 <sup>rd</sup> Order	SR>1.5	400–600	5–10 [sloping]	North	0.343–0.441	-2.841–[-0.959]
4 <sup>th</sup> Order		600–800	10–15 [moderately sloping]	Northeast	0.441–0.523	-0.959–0.687
		800–1000	15–30 [gently steep]	Northwest	0.523–0.624	0.687–2.803
		1000–1200	30–60 [steep]	South	0.624–0.765	2.803–6.566
		1200–1400	>60 [very steep]	Southwest	0.765–0.995	6.566–32.669
		1400–1600		Southeast		
		1600–1800		West		
		1800–2000				
	2000–2200					

et al., 2015). The determination of the number of groups is based on the experiment with different number of clusters.

Key terrain attributes such as elevation, slope, aspect, roughness, and curvature are providing a detailed understanding of the physical characteristics of the landscape, which are crucial for subsequent analysis. In other hand, the hydrological parameters help in understanding the river network’s hierarchy and its meandering nature. The terrain and river attributes are then grouped into two main clusters (Figure 2), one for terrain characteristics (Grouping V1) and another for river channel characteristics (Grouping V2).

Grouping version 1 includes river channel attributes where the river network is used as the base attribute, to which other attributes like the terrain attributes are added. These hydrological and terrain parameters may be grouped using statistical methods to identify similarities in channel characteristics which are visualized as raster lines. Grouping version 2 consists of terrain attributes only including elevation, slope, aspect, roughness, and curvature. These attributes are likely grouped also using statistical methods to identify similarities within the terrain data and are visualized as raster areas. Visualization in the form of raster areas makes the grouping results easier to see. In Grouping Version 3, land use land cover is used to verify how human intervention influences the physical parameters of the land surface, or how these parameters, in turn, affect human intervention.

## RESULTS

### Overall variable statistic

Three analyses were conducted on clustering version 1 using 7 parameters, clustering version 2 using 5 parameters, and version 3 using 6 parameters. The overall variable statistics presented in the analysis show the distribution and similarity of attributes across four groups, each characterized by different land surface parameters. The variables include river order, aspect, slope, curvature, elevation, terrain roughness index, channel sinuosity, and land use land cover. The box plots further illustrate the distribution and variance within each group, with some variables showing distinct separations across groups, while others display overlaps, reflecting the complexity and variability of the land surface characteristics being analyzed. This grouping analysis provides a structured way to classify the landscape into homogeneous zones, aiding in better understanding and management of the terrain, land cover, and hydrological features.

The distinct lines connecting the group centroids across the standardized values underscore the unique combination of characteristics within each group, reflecting their homogeneity in certain attributes while highlighting the variability in others. This differentiation is crucial for understanding and managing landscape features, as it allows for targeted analysis and decision-making based on the specific traits of each group. This visual representation using parallel box plot is a useful tool in

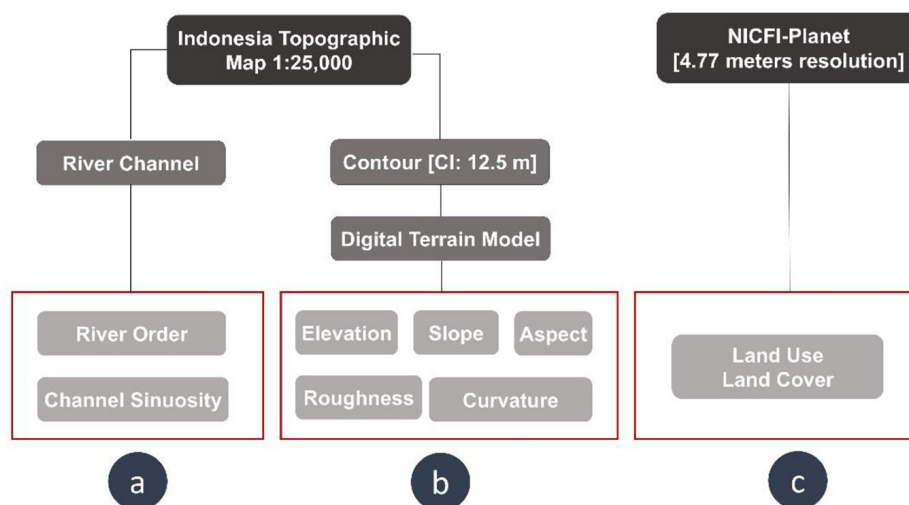


**Figure 2.** The main stages of land surface parameter grouping involve multivariate clustering, with clustering version 1 using parameters from groups a and b, clustering version 2 using parameters from group b only, and clustering version 3 using parameters from groups b and c

assessing how each parameter contributes to cluster formation, with parameters like elevation and slope standing out in terms of cluster differentiation. In all plots, the y-axis represents standardized values (ranging from -2 to 4), and the x-axis lists the analysis fields (parameters). Each line's colour corresponds to a different cluster, capturing variations in surface parameters across clusters.

Figure 3a shows clustering results with fewer clusters, likely representing the most basic categorization. Each line represents a distinct cluster (1–4). The standardized values fluctuate for each parameter, with elevation and slope parameters showing more variation across clusters. Figure 3b expands to five clusters (1–5). Here, additional clusters lead to more variance across parameters, especially in elevation and slope, highlighting differences between clusters in these parameters. Figure 3c represents seven clusters (1–7). The increase in clusters allows for finer distinctions among groups. There is noticeable differentiation in parameters like channel sinuosity, river order, and elevation. Figure 3d contains nine clusters (1–9), providing even more granular insights into how these parameters vary across clusters. The variance is most visible in the elevation and slope parameters, indicating these are influential in distinguishing between clusters.

Figure 4a comprising three clusters, this plot demonstrates a foundational level of segmentation. Clusters are depicted by lines of distinct colours (1–3). Elevation parameter exhibits the highest variance among clusters, indicating its

potential influence in differentiating the clusters. Other parameters, such as aspect and slope, display more uniformity across clusters. Five clusters (1–5) are presented in Figure 4b, expanding the range of cluster differentiation. Here, curvature and elevation parameters show more noticeable variations, with some clusters diverging significantly from others. This suggests that these parameters may provide useful distinctions when separating landscape features within these clusters. Figure 4c represents seven clusters, indicating a further refinement in cluster analysis. The addition of clusters introduces more variability across parameters, particularly for elevation, curvature, and slope. Such variations highlight the heterogeneity within the dataset, with elevation consistently emerging as a distinctive feature. The most granular clustering level in Figure 4d, this plot includes nine clusters. At this level, substantial fluctuations in the elevation and curvature parameters are observed, reflecting detailed differentiation. The increase in clusters reveals more subtle patterns in the data, making elevation and curvature dominant factors in defining clusters.

Three clusters from Figure 5a reveal moderate distinctions in curvature and slope, with notable overlaps in elevation and LULC. Five clusters in Figure 5b highlight increased variability, with curvature showing stronger separation and elevation remaining largely overlapped. Seven clusters from Figure 5c showcase more intricate patterns, with roughness and curvature exhibiting pronounced peaks and valleys. Nine clusters of

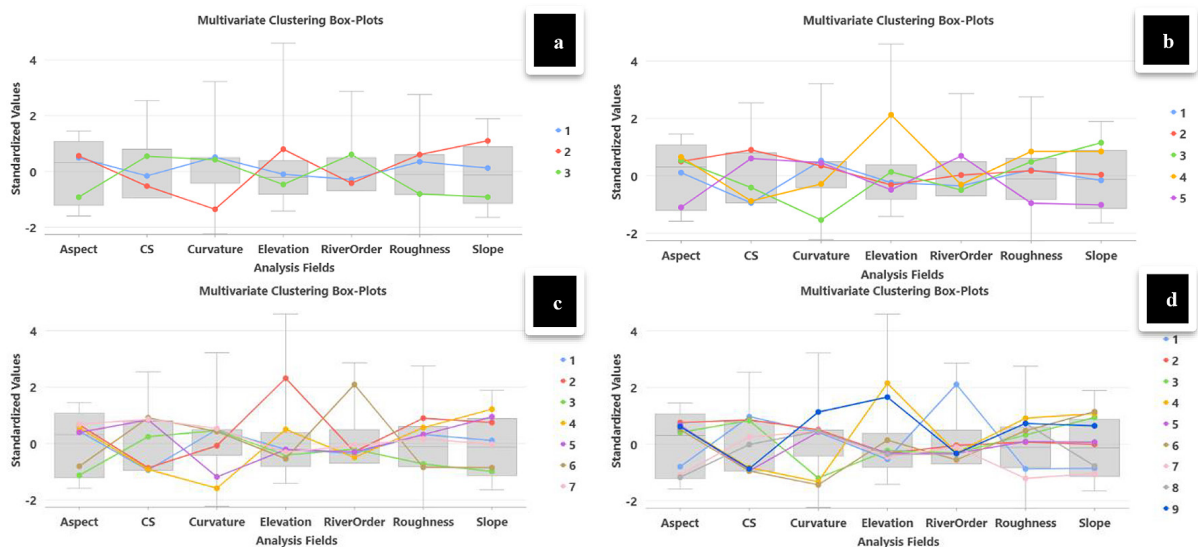


Figure 3. Parallel box plot from clustering version 1 using 7 parameters, comprising (a) 3 clusters, (b) 5 clusters, (c) 7 clusters, and (d) 9 clusters

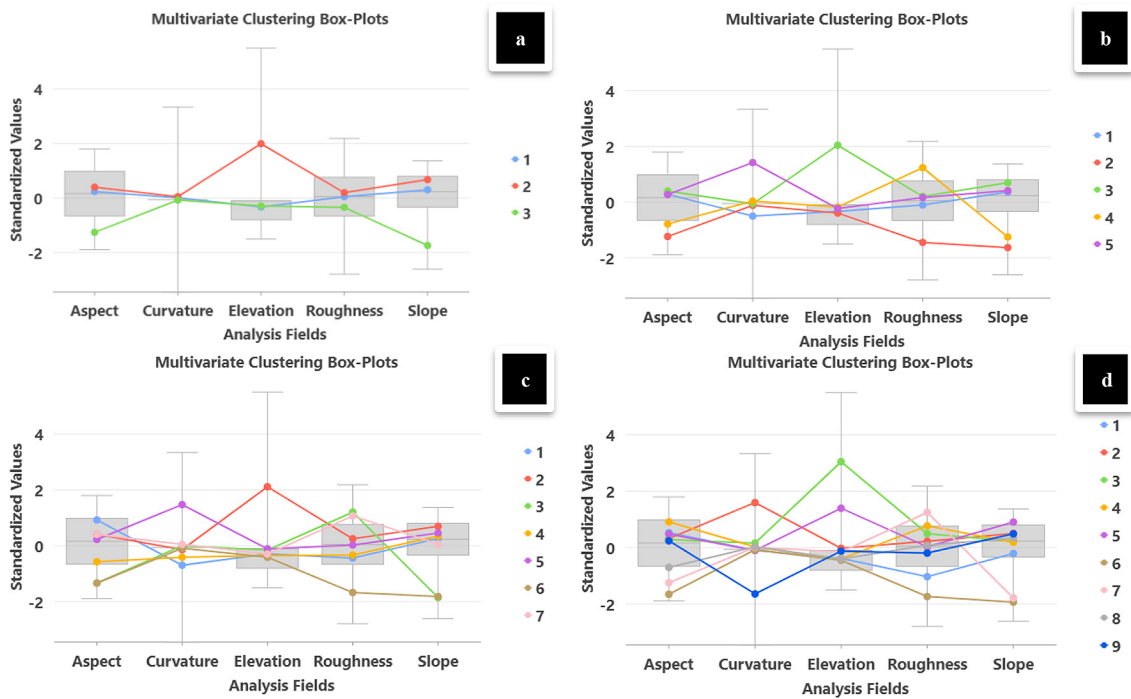


Figure 4. Parallel box plot from clustering version 2 using 5 parameters, comprising (a) 3 clusters, (b) 5 clusters, (c) 7 clusters, and (d) 9 clusters.

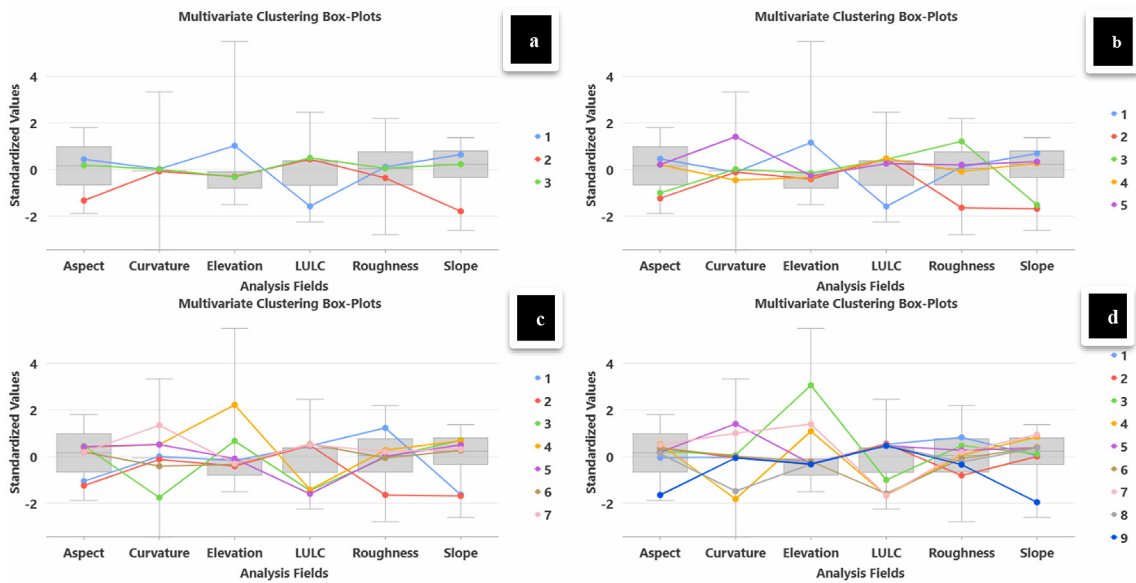
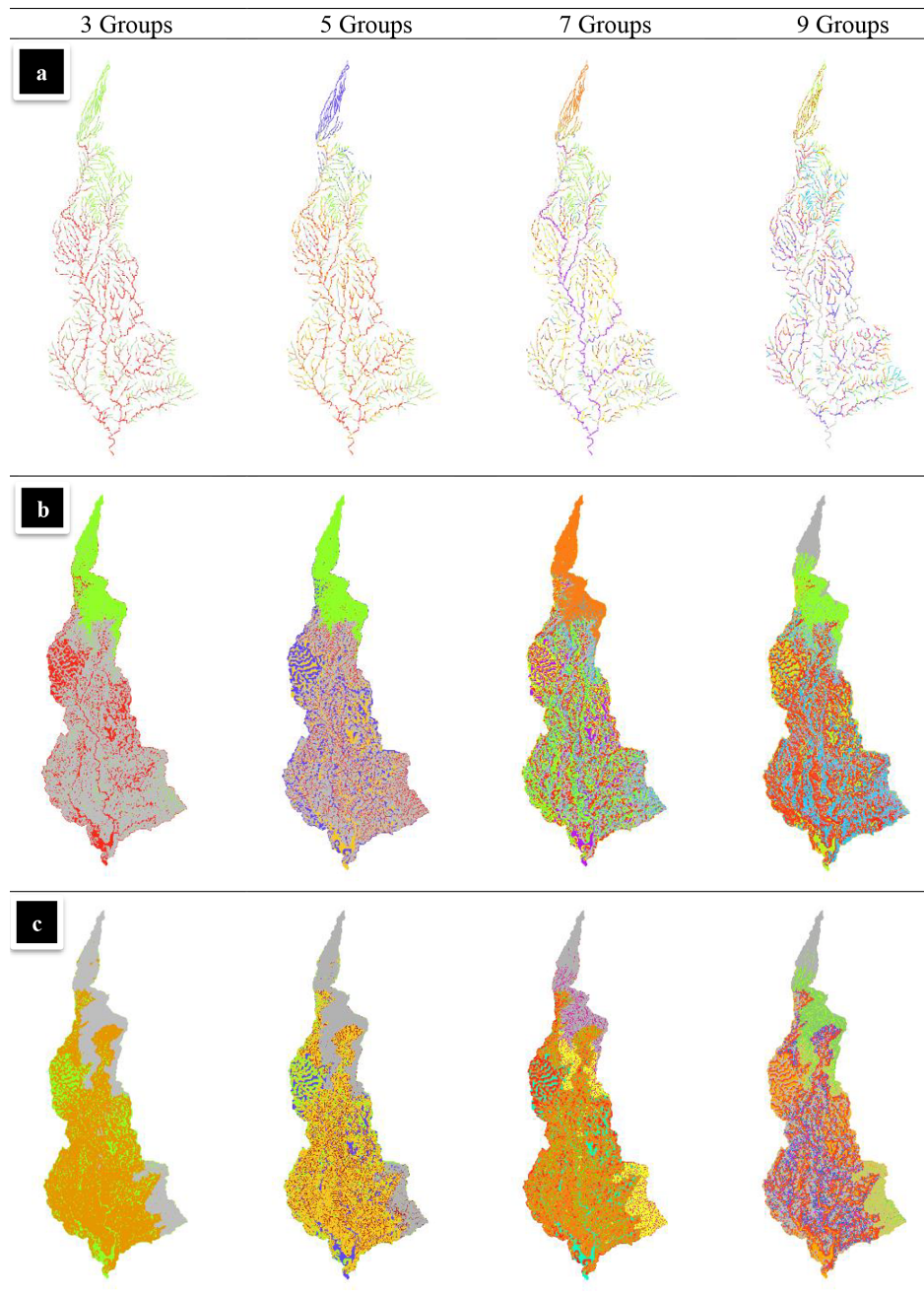


Figure 5. Parallel box plot from clustering version 3 using 6 parameters, comprising (a) 3 clusters, (b) 5 clusters, (c) 7 clusters, and (d) 9 clusters.

Figure 5d emphasize the complexity of land surface characteristics, with heightened variability in curvature and roughness while LULC remains consistent. As the number of clusters increases from 3 (graph a) to 9 (graph d), distinct separations emerge in variables like elevation, curvature, and roughness, highlighting their importance in group differentiation (Figure 5). Aspect

and LULC exhibit greater overlap across clusters, suggesting they contribute less to differentiation at these levels. As the number of clusters increases, the variance within each group decreases, and new patterns of separation emerge, particularly in the more distinct variables.

The spatial distribution of clusters mapped across the study area is presented in Figure 6a,



**Figure 6.** Map clustering version 1 using 7 parameters (6a), Figure 6b shows map clustering version 2 using 5 parameters, and map clustering version 3 using 6 parameters (6c).

utilizing seven surface parameters with river network as a basis analysis. Four maps are shown, each representing clustering results for 3, 5, 7, and 9 groups, respectively. Low order and high order Rivers start to appear at clustering 7 and 9 groups. Figure 6b illustrates spatial clustering results from Version 2 using five parameters (aspect, curvature, elevation, roughness, and slope) across four maps with 3, 5, 7, and 9 groups. Each map shows increasingly detailed segmentation, where more clusters capture finer variations in landscape characteristics. Starting with broad

distinctions in the 3-group map, the clustering becomes progressively granular, revealing complex, mosaic-like patterns in the 9-group map that highlight localized geomorphological features. How LULC influences the characterization of cluster diversity is illustrated in Figure 6c. As in Figure 6b, each map shows increasingly detailed segmentation with more detailed variations of 3, 5, 7, and 9 groups. The LULC parameter is very visible in influencing the homogeneity of the area in the upstream part of the watershed and the southern part downstream of the watershed.

The distinct color patterns in each map visually differentiate the clusters, thereby aiding in the interpretation of unique landscape characteristics associated with each grouping. This process enables a deeper understanding of the heterogeneity within the landscape, where each color represents a cluster characterized by a specific combination of surface parameters. This clustering approach, therefore, facilitates the identification of distinct zones or areas within the landscape, each exhibiting unique morphometric and topographic attributes. By examining the repetition and spatial arrangement of color patterns, distinctive landscape characteristics emerge, allowing for a refined delineation of the area.

### Re-delineation of mountain ecosystem units

The re-delineation of the landscape based on these repeated colour patterns provides a basis for defining landscape units that share similar geomorphological features. Additional parameter such as land use and land cover are a fundamental factor in delineating mountain ecosystems, affecting their ecological stability, biodiversity, and the provision of ecosystem services (Suescún et al., 2017). These landscape boundaries provide an overview of mountain ecosystem units. Such delineation is essential for ecological planning, land management, and conservation strategies, as it emphasizes the inherent variability within the landscape and allows for targeted interventions in each identified cluster zone.

Spatially, by using expert judgement, the repetitive pattern of distinctly clustered colors can be delineated iconically. In this study, based on the recurring patterns observed, five landscape units were identified, reflecting the ecosystems of Mount Sumbing within the Kodil Watershed area. These units include: (1) young Sumbing volcanic peak ecosystem, (2) old Sumbing volcanic peak ecosystem, (3) old Sumbing volcanic slope ecosystem, (4) transitional volcanic ecosystem, and (5) old Menoreh volcanic ecosystem.

Based on the findings from the clustering of surface parameters, the ecosystem of the young Sumbing volcanic peak exhibits dominant slope orientations toward the south, southeast, and southwest. The curvature of this area is characterized by significantly negative values, indicating the presence of deep valleys along volcanic lahar flow paths. The roughness index in Area 1 is predominantly positive (0.523–0.765), reflecting

a moderately rugged surface. Elevation parameters are more discernible, with Area 1 situated at an elevation range of 1,600–2,200 m above sea level. Slope variation in this area ranges from 15% to 60% (gently steep to very steep). From the perspective of river characteristics, Area 1 is dominated by first-order streams with low sinuosity values, representing straight river flows typical of the headwaters of the Kodil Watershed.

The ecosystem of old Sumbing volcanic peak is characterized by dominant slope orientations toward the east, southeast, west, and southwest. The topographical index of Area 2 reveals a balanced distribution between deep valleys and sharp mountain ridges, reflecting the intensive erosion processes that have shaped the older volcanic formation of Mount Sumbing. The roughness index in Area 2 predominantly falls within the intermediate range (0.343–0.523), indicating a moderately rugged surface. The elevation of this area ranges from 800 to 1,600 m above sea level (asl). The slope angles of the landscape are between 30% and 60% (steep to very steep). The river network in Area 2 begins to exhibit meandering flows, with sinuosity values ranging from 1.1 to 1.5, although some straight river channels can still be observed in the upstream sections.

The ecosystem of the slopes of the older volcanic formation of Mount Sumbing exhibits slope orientations like its summit ecosystem, with dominant directions toward the east, southeast, west, and southwest. The elevation of Area 3 spans a range of 600–800 m above sea level (asl), featuring gently sloping to steep gradients (5%–60%). The roughness index for this area is moderate, with values ranging from 0.343 to 0.523. The river network in Area 3 is characterized by moderate sinuosity (SR 1.1–1.5) and includes streams ranging from first to third order.

The transitional volcanic ecosystem is characterized by predominantly flat slope orientations, with some slopes facing east, south, and southeast. The curvature of this area is primarily flat, ranging from -0.959 to 0.687, indicating that the surface has received volcanic material deposits from higher elevations. The roughness index in this area shows a balanced distribution, dominated by both low roughness values (<0.211) and high roughness values (0.765–0.995), covering a significant extent of the area. Area 4 spans an elevation range of 400–800 m above sea level (asl). The slope angles in this area exhibit distinct variations, ranging from flat to moderately sloping.

The river network in Area 4 is characterized by moderate to high meandering flows, with sinuosity values of 1.1–1.5. However, the river flow directions remain consistently from the north.

The ecosystem of the old volcanic of Menoreh is dominated by slope orientations toward the east, southeast, and south. The curvature index of Area 4 displays a balanced distribution between valleys and hill ridges, reflecting processes of erosion and deposition. The roughness index in this area is evenly distributed, ranging from the lowest to the highest values. Area 4 has the lowest elevation, spanning 200–400 m above sea level (asl). The slope variation in this landscape ranges from flat to very steep. Area 4 features a river network with stream orders ranging from 1 to 4, exhibiting the highest sinuosity overall. However, the upstream river catchment areas still have low sinuosity. Unlike other areas, the first-order streams in this region originate from two distinct directions: north and south.

## DISCUSSION

The relationship between subsurface and land surface conditions is illustrated in Figure 7. The geological unit pattern (Figure 7a) represents the types

and distribution of rocks formed through processes such as sedimentation, deformation, and magma intrusion in the past (Burbank and Anderson, 2011; Carter, 2011; Huggett, 2016). This geological setting reflects the area’s geological history, including volcanic activity (igneous rocks), sedimentation in marine or fluvial environments (sedimentary rocks), and transformations caused by high pressure and temperature (metamorphic rocks). In contrast, Figure 7b provides a detailed depiction of current land surface conditions, highlighting information such as elevation, slope angle variations, slope orientation, roughness and surface curvature indices, and river sinuosity patterns. Lastly, current situation of the land surface covering by its land use indicates how land potential and limitations affect humans in utilizing existing resources.

The utilization of land resource potential focuses more on current land surface conditions rather than solely on the processes of past rock formation. These surface conditions serve as a foundation for identifying both the potential and limitations of land use (Reddy, 2018). However, present surface characteristics are intrinsically linked to historical processes. For instance, eruptions from the older and younger Sumbing volcanoes deposited volcanic fallout and sediment, which now constitute the surrounding surface material.

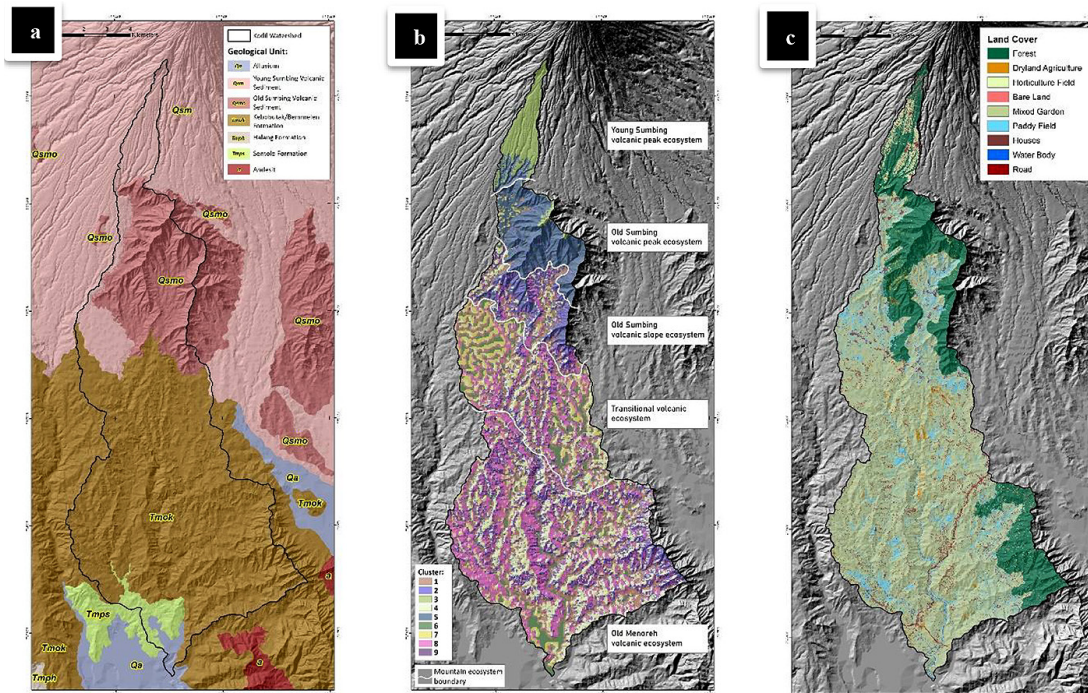


**Figure 7.** Geological setting of the study area describes subsurface condition (a), mountain ecosystem units in Kodil watershed represents the surface parameters influencing by its subsurface material then interact with the land utilization, and land use land cover shows the human intervention in utilizing the potential of land resources (c)

The landscape influenced by material from young volcanic eruptions is most evident in the young Sumbing volcanic ecosystem, characterized by its highest elevations, steep south-facing slopes, and low-order rivers flowing straight to the south. In contrast, the older Sumbing volcanic ecosystem exhibits a higher degree of surface roughness, attributed to earlier, more intense volcanic activity and prolonged geomorphological processes of erosion and deposition.

The direction and deposition of material from the eruptions of the older and younger Sumbing volcanoes in the past were not confined to the Qsm and Qsmo formations (Figure 7a). Previous surface material analyses reveal that volcanic fallout and deposits from both the older and younger Sumbing volcanoes also spread over and overlapped the Tmok formation, with a thickness exceeding 2 meters (Noviyanto et al., 2020; Pratiwi et al., 2019; Pulungan and Sartohadi, 2018; Sartohadi et al., 2018; Wida et al., 2019). The processes that formed the Tmok formation differ significantly from those that created the younger volcanic materials of Qsm and Qsmo, giving the transitional volcanic ecosystem a unique and distinct character. The old Menoreh volcanic ecosystem (Tmok) occupies the largest area within the Kodil watershed. A significant uniformity in land surface parameters is the river flow patterns, which originate not only from the north but also from the east, south, and west. The erosional-depositional relief is highly pronounced, as seen in the varying surface roughness between hilltops and narrow valleys.

It can be highlighted that the complexity of ecosystems is not fully detailed in geological maps, which primarily emphasize subsurface material information. However, surface geomorphological processes, combined with historical material displacement, can be analyzed using the principles of superposition and spatial arrangement (Ford et al., 2014; Kooi and Beaumont, 1996). The uniformity patterns of land surface characteristics are illustrated in the clustering results shown in Figure 7b. These patterns, which define ecosystem units, are more easily identified and observed iconically in the field. Each ecosystem unit provides clearer insights into land potential, reflecting its ecosystem services, as well as the factors that limit its use. Land potential and limitations are interrelated, requiring strategies to maximize potential while minimizing constraints, thereby enabling sustainable land management.

Altitude influences the selection of suitable plant types, rainfall patterns, and microclimatic temperatures (Opedal et al., 2015). Steep slopes are more prone to erosion, whereas gentle slopes provide greater stability for human activities. In high-altitude areas, measures such as terracing or planting erosion-resistant vegetation can be implemented to mitigate risks (Walia et al., 2024). This can be seen from the land cover at high altitudes which is still forest (Figure 7c). Slope direction affects solar radiation intensity and moisture distribution. Sun-facing slopes (south-facing in the northern hemisphere and north-facing in the southern hemisphere) tend to be hotter and drier. Conversely, slopes facing away from the sun (north-facing in the northern hemisphere and south-facing in the southern hemisphere) receive higher solar intensity, making them suitable for plants requiring abundant sunlight (Cheng et al., 2023). Southwest-facing slopes are generally wetter, favoring plants with high water needs. At the study location, the upstream area of the watershed with a south-facing slope is widely used as a horticulture field area. Slope-related limitations can be mitigated through microclimate engineering to optimize sunlight utilization on less exposed slopes. Steep slope angles increase erosion risks and accessibility challenges, which can be addressed through contour-based land management systems to reduce erosion.

The roughness index reflects the degree of micro-topographic variability, while curvature indicates surface concavity or convexity (Hoechstetter et al., 2008; Tarolli, 2014). High roughness suggests uneven surfaces often linked to erosion and drainage issues. Conversely, low roughness areas are more stable and suitable for settlements or intensive agriculture. Areas with low roughness in the study site are mostly used for paddy fields, while locations with high roughness have land cover in the form of mixed gardens and dryland agriculture. Concave curvature zones (convergent) are ideal for water catchment, while convex zones (divergent), which are prone to erosion, can benefit from slope stabilization techniques. Most settlements occupy convex zone locations, which can increase the accumulation of surface flow and trigger erosion, landslides, and flash floods. Surface flow control is necessary to minimize the impact of its power. Meanwhile in the valley-concave section can be optimized with drainage and reservoir systems.

Rivers of higher order exhibit distinct characteristics compared to lower-order streams.

Lower-order rivers, typically located upstream, are straighter and offer potential for clean water supply and biodiversity conservation. These areas can be managed for erosion control through vegetation retention. Mid-order rivers, where flows become more meandering, are suitable for irrigation and agroforestry due to stable discharge, although local flooding risks must be addressed. High-order rivers downstream present opportunities for fisheries and wetland agriculture, leveraging their water resources effectively (Ran et al., 2022).

## CONCLUSIONS

What is visible on the earth's surface today does not always correspond to the information depicted on geological maps, which primarily represent subsurface features. The morphology of the current land surface is shaped by the interplay of past volcanic-tectonic processes with the present of erosion-deposition. National topographic maps serve as a primary data source for delineating mountain ecosystems. Derivative data, such as river order, channel sinuosity, elevation, slope, aspect, roughness index, and curvature, provide land surface attributes that can be grouped based on spatial patterns. Land use and land cover data are additional parameters to see the reciprocal relationship between land surface parameters and human intervention living on it. These repeated attributes are visually distinct and can be used to draw boundaries iconically. These boundaries offer valuable references for local spatial planning. Land surface attributes reflect both the potential and limitations of land resources. By analyzing the interplay and influence of these parameters, potential can be optimized while limitations are minimized, enabling sustainable land resource management.

## Acknowledgements

This research is independent research that does not receive financial support from any party.

## REFERENCES

- Antonelli, A., Kissling, W. D., Flantua, S. G. A., Bermúdez, M. A., Mulch, A., Muellner-Riehl, A. N., Kreft, H., Linder, H. P., Badgley, C., Fjeldså, J., Fritz, S. A., Rahbek, C., Herman, F., Hooghiemstra, H., and Hoorn, C. (2018). Geological and climatic influences on mountain biodiversity. *Nature Geoscience*, 11(10). <https://doi.org/10.1038/s41561-018-0236-z>
- Apriadsa, A., Anggoro, H. S., Cahyono, A., and Apriadna, R. (2019). Unveil the 'lost toponyms' in the northern part of the Menoreh Mountains, Java, Indonesia. *International Journal of Cartography*, 5(2–3). <https://doi.org/10.1080/23729333.2019.1611025>
- Aspinall, R., and Pearson, D. (2000). Integrated geographical assessment of environmental condition in water catchments: Linking landscape ecology, environmental modelling and GIS. *Journal of Environmental Management*, 59(4), 299–319. <https://doi.org/10.1006/JEMA.2000.0372>
- Belyanin, P. S. (2021). The landscape structure of the Gede–Pangrango Stratovolcano (West Java, Indonesia). *Geography and Natural Resources*, 42(4). <https://doi.org/10.1134/S187537282104003X>
- Birkeland, P. (2014). Mountain geography: Physical and human dimensions. Edited by Martin F. Price, Alton C. Byers, Donald A. Friend, Thomas Kohler, and Larry W. Price. *Arctic, Antarctic, and Alpine Research* 46(2). <https://doi.org/10.1657/1938-4246-46.2.525>
- Bishop, M. P., and Dobreva, I. D. (2017). *Geomorphometry and mountain geodynamics: Issues of scale and complexity*. Integrating Scale in Remote Sensing and Gis. <https://doi.org/10.1201/9781315373720-17>
- Burbank, D. W., and Anderson, R. S. (2011). *Tectonic geomorphology*: Second Edition. In *Tectonic Geomorphology: Second Edition*. <https://doi.org/10.1002/9781444345063>
- Carter, A. (2011). R. S. Anderson and S. P. Anderson 2010. *Geomorphology: The Mechanics and Chemistry of Landscapes*. xvi + 637pp. Cambridge University Press. Price £40.00, US\$75.00 (PB). ISBN 978 0 521 51978 6. *Geological Magazine*, 148(2). <https://doi.org/10.1017/s0016756810000932>
- Chen, J. (2002). Landscape ecology: A top–down approach. *Ecological Engineering*, 18(4). [https://doi.org/10.1016/s0925-8574\(02\)00006-x](https://doi.org/10.1016/s0925-8574(02)00006-x)
- Cheng, Z., Aakala, T., and Larjavaara, M. (2023). Elevation, aspect, and slope influence woody vegetation structure and composition but not species richness in a human-influenced landscape in northwestern Yunnan, China. *Frontiers in Forests and Global Change*, 6. <https://doi.org/10.3389/ffgc.2023.1187724>
- Clements, B., Hall, R., Smyth, H. R., and Cottam, M. A. (2009). Thrusting of a volcanic arc: A new structural model for Java. *Petroleum Geoscience*, 15(2). <https://doi.org/10.1144/1354-079309-831>
- Cullingham, C. I., Janes, J. K., Hamelin, R. C., James, P. M. A., Murray, B. W., and Sperling, F. A. H. (2019). The contribution of genetics and genomics to understanding the ecology of the mountain pine beetle system. *Canadian Journal of Forest Research*, 49(7). <https://doi.org/10.1139/cjfr-2018-0303>

13. Ford, J. R., Price, S. J., Cooper, A. H., and Waters, C. N. (2014). An assessment of lithostratigraphy for anthropogenic deposits. *Geological Society Special Publication*, 395(1). <https://doi.org/10.1144/SP395.12>
14. Fouedjio, F., and Arya, E. (2024). Locally varying geostatistical machine learning for spatial prediction. *Artificial Intelligence in Geosciences*, 5, 100081. <https://doi.org/10.1016/J.AIIG.2024.100081>
15. García-Navas, V., Sattler, T., Schmid, H., and Ozgul, A. (2020). Temporal homogenization of functional and beta diversity in bird communities of the Swiss Alps. *Diversity and Distributions*, 26(8). <https://doi.org/10.1111/ddi.13076>
16. Germino, M. J., Reiners, W. A., Blasko, B. J., McLeod, D., and Bastian, C. T. (2001). Estimating visual properties of Rocky Mountain landscapes using GIS. *Landscape and Urban Planning*, 53(1–4), 71–83. [https://doi.org/10.1016/S0169-2046\(00\)00141-9](https://doi.org/10.1016/S0169-2046(00)00141-9)
17. Giano, S. I., Danese, M., Gioia, D., Pescatore, E., Siervo, V., and Bentivenga, M. (2020). *Tools for Semi-automated Landform Classification: A Comparison in the Basilicata Region* (Southern Italy). Lecture Notes in Computer Science (Including Subseries Lecture Notes in Artificial Intelligence and Lecture Notes in Bioinformatics), 12250 LNCS. [https://doi.org/10.1007/978-3-030-58802-1\\_51](https://doi.org/10.1007/978-3-030-58802-1_51)
18. Grêt-Regamey, A., Bebi, P., Bishop, I. D., and Schmid, W. A. (2008). Linking GIS-based models to value ecosystem services in an Alpine region. *Journal of Environmental Management*, 89(3), 197–208. <https://doi.org/10.1016/J.JENVMAN.2007.05.019>
19. Grêt-Regamey, A., Brunner, S. H., and Kienast, F. (2012). Mountain ecosystem services: Who cares? *Mountain Research and Development*, 32(SUPPL. 1). <https://doi.org/10.1659/MRD-JOURNAL-D-10-00115.S1>
20. Grêt-Regamey, A., and Weibel, B. (2020). Global assessment of mountain ecosystem services using earth observation data. *Ecosystem Services*, 46, 101213. <https://doi.org/10.1016/J.ECOSER.2020.101213>
21. Hoehstetter, S., Walz, U., Dang, L. H., and Thinh, N. X. (2008). Effects of topography and surface roughness in analyses of landscape structure - A proposal to modify the existing set of landscape metrics. *Landscape Online*, 3(1). <https://doi.org/10.3097/LO.200803>
22. Huggett, R. J. (2016). *Fundamentals of Geomorphology*. In *Fundamentals of Geomorphology*. <https://doi.org/10.4324/9781315674179>
23. Kang, Y., Wu, K., Gao, S., Ng, I., Rao, J., Ye, S., Zhang, F., and Fei, T. (2022). STICC: a multivariate spatial clustering method for repeated geographic pattern discovery with consideration of spatial contiguity. *International Journal of Geographical Information Science*, 36(8). <https://doi.org/10.1080/13658816.2022.2053980>
24. Karki, S., Webb, J. A., Stewardson, M. J., Fowler, K., and Kattel, G. R. (2023). Basin-scale riverine ecosystem services vary with network geometry. *Ecosystem Services*, 63. <https://doi.org/10.1016/j.ecoser.2023.101555>
25. Kooi, H., and Beaumont, C. (1996). Large-scale geomorphology: Classical concepts reconciled and integrated with contemporary ideas via a surface processes model. *Journal of Geophysical Research: Solid Earth*, 101(2). <https://doi.org/10.1029/95jb01861>
26. Körner, C. (2021). Alpine plant life: Functional plant ecology of high mountain ecosystems. In *Alpine Plant Life: Functional Plant Ecology of High Mountain Ecosystems*. <https://doi.org/10.1007/978-3-030-59538-8>
27. Lane, B. A., Pasternack, G. B., Dahlke, H. E., and Sandoval-Solis, S. (2017). The role of topographic variability in river channel classification. *Progress in Physical Geography*, 41(5). <https://doi.org/10.1177/0309133317718133>
28. Lauder, M. R. M. T., Bachtiar, T., and Sobarna, C. (2023). *Geographical Names as Indicators of the Environment: Case Study in Bandung Basin, West Java, Indonesia*. In *Key Challenges in Geography: Vol. Part F2248*. [https://doi.org/10.1007/978-3-031-21510-0\\_26](https://doi.org/10.1007/978-3-031-21510-0_26)
29. Li, A., Wang, A., Liang, S., and Zhou, W. (2006). Eco-environmental vulnerability evaluation in mountainous region using remote sensing and GIS—A case study in the upper reaches of Minjiang River, China. *Ecological Modelling*, 192(1–2), 175–187. <https://doi.org/10.1016/J.ECOLMODEL.2005.07.005>
30. MacMillan, R. A., Jones, R. K., and McNabb, D. H. (2004). Defining a hierarchy of spatial entities for environmental analysis and modeling using digital elevation models (DEMs). *Computers, Environment and Urban Systems*, 28(3), 175–200. [https://doi.org/10.1016/S0198-9715\(03\)00019-X](https://doi.org/10.1016/S0198-9715(03)00019-X)
31. Marti, E., Leray, S., Vilella, D., Maringue, J., Yáñez, G., Salazar, E., Poblete, F., Jimenez, J., Reyes, G., Poblete, G., Huamán, Z., Figueroa, R., Araya Vargas, J., Sanhueza, J., Muñoz, M., Charrier, R., and Fernández, G. (2023). Unravelling geological controls on groundwater flow and surface water-groundwater interaction in mountain systems: A multi-disciplinary approach. *Journal of Hydrology*, 623. <https://doi.org/10.1016/j.jhydrol.2023.129786>
32. Mileyko, Y., Edelsbrunner, H., Price, C. A., and Weitz, J. S. (2012). Hierarchical ordering of reticular networks. *PLoS ONE*, 7(6). <https://doi.org/10.1371/journal.pone.0036715>
33. Minár, J., and Evans, I. S. (2008). Elementary forms for land surface segmentation: The theoretical basis of terrain analysis and geomorphological mapping.

- Geomorphology*, 95(3–4). <https://doi.org/10.1016/j.geomorph.2007.06.003>
34. Noviyanto, A., Sartohadi, J., and Purwanto, B. H. (2020). The distribution of soil morphological characteristics for landslide-impacted Sumbing Volcano, Central Java - Indonesia. *Geoenvironmental Disasters*, 7(1). <https://doi.org/10.1186/S40677-020-00158-8>
  35. Oberle, P., Ikhwan, M., Stoffel, D., and Nestmann, F. (2016). Adapted hydropower-driven water supply system: assessment of an underground application in an Indonesian karst area. *Applied Water Science*, 6(3). <https://doi.org/10.1007/s13201-016-0425-0>
  36. Opedal, Ø. H., Armbruster, W. S., and Graae, B. J. (2015). Linking small-scale topography with microclimate, plant species diversity and intra-specific trait variation in an alpine landscape. *Plant Ecology and Diversity*, 8(3). <https://doi.org/10.1080/17550874.2014.987330>
  37. Pannekoek, A. (1949). *Outline of the Geomorphology of Java*. TAG: The Netherlands. [https://scholar.google.co.id/scholar?hl=en&andas\\_sdt=0%2C5andq=Pannekoek+1949+Geomorphology+of+JavaandbtnG=](https://scholar.google.co.id/scholar?hl=en&andas_sdt=0%2C5andq=Pannekoek+1949+Geomorphology+of+JavaandbtnG=)
  38. Patley, M. K., Tiwari, A., Kumar, K., Arumugam, T., Kinattinkara, S., and Arumugam, M. (2024). Study of mountain ecosystem accounting in lower Himalaya range in Uttarakhand, India using geospatial technology. *Results in Engineering*, 21. <https://doi.org/10.1016/j.rineng.2024.101811>
  39. Patru-Stupariu, I., Hossu, C. A., Gradinaru, S. R., Nita, A., Stupariu, M. S., Huzui-Stoiculescu, A., and Gavrilidis, A. A. (2020). A review of changes in mountain land use and ecosystem services: From theory to practice. *Land*, 9(9). <https://doi.org/10.3390/LAND9090336>
  40. Peeters, A., Zude, M., Käthner, J., Ünlü, M., Kanber, R., Hetzroni, A., Gebbers, R., and Ben-Gal, A. (2015). Getis-Ord's hot- and cold-spot statistics as a basis for multivariate spatial clustering of orchard tree data. *Computers and Electronics in Agriculture*, 111. <https://doi.org/10.1016/j.compag.2014.12.011>
  41. Pratiwi, E. S., Sartohadi, J., and Wahyudi. (2019). Geoelectrical Prediction for Sliding Plane Layers of Rotational Landslide at the Volcanic Transitional Landscapes in Indonesia. *IOP Conference Series: Earth and Environmental Science*, 286(1). <https://doi.org/10.1088/1755-1315/286/1/012028>
  42. Prskalo, G. (2010). Improved Horton-Strahler scheme for stream network classification and its implementation in the method of geomorphologic instantaneous unit hydrograph. *Journal of Environmental Hydrology*, 18.
  43. Pulungan, N. A., and Sartohadi, J. (2018). New Approach to Soil Formation in the Transitional Landscape Zone: Weathering and Alteration of Parent Rocks. *Journal of Environments*, 5(1). <https://doi.org/10.20448/journal.505.2018.51.1.7>
  44. Ran, Y., Liu, Y., Wu, S., Li, W., Zhu, K., Ji, Y., Mir, Y., Ma, M., and Huang, P. (2022). A higher river sinuosity increased riparian soil structural stability on the downstream of a dammed river. *Science of the Total Environment*, 802. <https://doi.org/10.1016/j.scitotenv.2021.149886>
  45. Reddy, G. P. O. (2018). *Geospatial Technologies in Land Resources Mapping, Monitoring, and Management: An Overview*. [https://doi.org/10.1007/978-3-319-78711-4\\_1](https://doi.org/10.1007/978-3-319-78711-4_1)
  46. Salvacion, A. R. (2016). Terrain characterization of small island using publicly available data and open-source software: a case study of Marinduque, Philippines. *Modeling Earth Systems and Environment*, 2(1). <https://doi.org/10.1007/s40808-016-0085-y>
  47. Šamanović, S., Medak, D., and Gajski, D. (2016). *Analysis Of The Pit Removal Methods In Digital Terrain Models Of Various Resolutions*. The International Archives of the Photogrammetry, Remote Sensing and Spatial Information Sciences, XLI-B2. <https://doi.org/10.5194/isprs-archives-xli-b2-235-2016>
  48. Saputra, A., Gomez, C., Delikostidis, I., Zawar-Reza, P., Hadmoko, D. S., Sartohadi, J., and Setiawan, M. A. (2018). Determining earthquake susceptible areas southeast of yogyakarta, Indonesia—outcrop analysis from structure from motion (SfM) and geographic information system (GIS). *Geosciences (Switzerland)*, 8(4). <https://doi.org/10.3390/geosciences8040132>
  49. Sartohadi, J., Harlin Jennie Pulungan, N. A., Nurudin, M., and Wahyudi, W. (2018). The ecological perspective of landslides at soils with high clay content in the middle bogowonto watershed, central Java, Indonesia. *Applied and Environmental Soil Science*, 2018. <https://doi.org/10.1155/2018/2648185>
  50. Sathyamoorthy, D. (2009). Computation of scale independent surface roughness. *Defence Sand Technical Bulletin*, 2(1).
  51. Skoulikidis, N. T. (2021). *Mountainous areas and river systems*. In Environmental Water Requirements in Mountainous Areas. <https://doi.org/10.1016/B978-0-12-819342-6.00009-9>
  52. Suescún, D., Villegas, J. C., León, J. D., Flórez, C. P., García-Leoz, V., and Correa-Londoño, G. A. (2017). Vegetation cover and rainfall seasonality impact nutrient loss via runoff and erosion in the Colombian Andes. *Regional Environmental Change*, 17(3). <https://doi.org/10.1007/s10113-016-1071-7>
  53. Tarolli, P. (2014). High-resolution topography for understanding Earth surface processes: Opportunities and challenges. *Geomorphology*, 216, 295–312. <https://doi.org/10.1016/J.GEOMORPH.2014.03.008>
  54. Tefera, G. W., Ray, R. L., and Bantider, A. (2024).

- Exploring the unique biophysical characteristics and ecosystem services of mountains: A review. *Journal of Mountain Science*, 21(11), 3584–3597. <https://doi.org/10.1007/S11629-024-8828-0/METRICS>
55. Van Bemmelen, R. W. (1949). *The Geology of Indonesia. General Geology of Indonesia and Adjacent Archipelagoes*. In Government Printing Office, The Hague.
56. Walia, S. S., Kaur, K., and Kaur, T. (2024). *Soil and Water Conservation Techniques in Rainfed Areas*. In Rainfed Agriculture and Watershed Management. [https://doi.org/10.1007/978-981-99-8425-1\\_15](https://doi.org/10.1007/978-981-99-8425-1_15)
57. Weiss, D. J., and Walsh, S. J. (2009). Remotesensing of mountain environments. *Geography Compass*, 3(1). <https://doi.org/10.1111/j.1749-8198.2008.00200.x>
58. West, N. (2001). Spatial Pattern Analysis in Plant Ecology. *Crop Science*, 41(3). <https://doi.org/10.2135/cropsci2001.413916x>
59. Wida, W. A., Maas, A., and Sartohadi, J. (2019). Pedogenesis of Mt. Sumbing Volcanic Ash above The Alteration Clay Layer in The Formation of Landslide Susceptible Soils in Bompon Sub-Watershed. *Ilmu Pertanian (Agricultural Science)*, 4(1). <https://doi.org/10.22146/ipas.41893>
60. Zhang, P., Yao, W., Tang, H., and Xiao, P. (2018). Rill morphology change and its effect on erosion and sediment yield on loess slope. *Nongye Gongcheng Xuebao/Transactions of the Chinese Society of Agricultural Engineering*, 34(5). <https://doi.org/10.11975/j.issn.1002-6819.2018.05.015>
61. Zhou, D., and Song, W. (2021). Identifying ecological corridors and networks in mountainous areas. *International Journal of Environmental Research and Public Health*, 18(9). <https://doi.org/10.3390/ijerph18094797>